applied sciences

MDPI

Article

Regeneration of Activated Carbons Spent by Waste Water Treatment Using KOH Chemical Activation

Jung Eun Park, Gi Bbum Lee, Bum Ui Hong and Sang Youp Hwang *

Plant Engineering Division, Institute for Advanced Engineering, Yongin-si 17180, Korea; jepark0123@gmail.com (J.E.P.); mnbbv21c@gmail.com (G.B.L.); buhong@iae.re.kr (B.U.H.)
* Correspondence: syhwang80@gmail.com; Tel.: +82-31-330-7271

Received: 29 October 2019; Accepted: 22 November 2019; Published: 27 November 2019

Abstract: In this study, spent activated carbons (ACs) were collected from a waste water treatment plant (WWTP) in Incheon, South Korea, and regenerated by heat treatment and KOH chemical activation. The specific surface area of spent AC was 680 m^2/g, and increased up to 710 m^2/g through heat treatment. When the spent AC was activated by the chemical agent potassium hydroxide (KOH), the surface area increased to 1380 m^2/g. The chemically activated ACs were also washed with acetic acid (CH_3COOH) to compare the effect of ash removal during KOH activation. The low temperature N_2 adsorption was utilized to measure the specific surface areas and pore size distributions of regenerated ACs by heat treatment and chemical activation. The functional groups and adsorbed materials on ACs were also analyzed by X-ray photoelectron spectroscopy and X-ray fluorescence. The generated ash was confirmed by proximate analysis and elementary analysis. The regenerated ACs were tested for toluene adsorption, and their capacities were compared with commercial ACs. The toluene adsorption capacity of regenerated ACs was higher than commercial ACs. Therefore, it is a research to create high value-added products using the waste.

Keywords: activated carbon; KOH; regeneration; heat treatment; chemical activation; toluene adsorption; ash removal

1. Introduction

Activated carbons (ACs) have been widely used for the water treatment process, which includes the removal of odors, heavy metals, and organic compounds. In particular, drinking water treatment plants (DWTP) and waste water treatment plants (WWTP) require various types of ACs in large quantities [1–3]. Granular activated carbon (GAC) is commonly used in the filtration process of DWTP [2,4]. This process can effectively remove organic matter, taste and odor-causing compounds. Powdered activated carbon (PAC) is usually used in final stage of WWTP. The treated water should meet the stringent effluent standard before discharging the water to the river. The PAC filtration process efficiently removes pollutants, so should be required in the WWTP [1,2].

Water treatment plants require a large amount of fresh ACs, but this means that large amounts of spent ACs could be generated after losing the adsorption capacity. The spent ACs are classified into hazardous solid wastes, and are thus prohibited to dispose directly into landfill sites [5,6]. The regeneration of ACs is more economically and environmentally effective than replacing fresh ACs [7,8]. Various regeneration methods have been investigated, including wet oxidation, classical solvent regeneration, and thermal regeneration [9]. Thermal regeneration in particular has been widely used due to its simplicity, low cost, and versatility [7,10,11].

During thermal regeneration, spent ACs are exposed to high temperatures (~850 °C) in the inert gas, and followed by oxidizing conditions [12]. When thermally heated, any volatile compounds adsorbed in the pores are eliminated, and less-volatile compounds are decomposed [3,5]. Thus, the specific

surface area and pores of spent ACs are efficiently regenerated [13]. The surface area of spent ACs using heat treatments was observed to increase compared with their initial surface area of untreated spent ACs [3,14]. This is because metals accumulating in pores and surface during the water purification process could react as catalysts at a high temperature. The accumulation of metals catalyzes the reaction between surface carbon and oxidizing agents, leading to a pore development and increased surface area.

Thermal regeneration of spent ACs usually results in a lower carbon yield and ash generation [15]. This in turn leads to a negative effect of AC regeneration. The oxidative reaction at high temperatures results in the pyrolysis of the surface carbons, which are then gasified and evaporate, leading to the low carbon yield [3,15]. Ashes are generated during the thermal treatment which usually block the pores and covers the carbon surface [16]. While the carbon atoms on the exposed surface can be used the active site for adsorption, the ashes covering the surface will reduce the active sites, as well as the adsorption capacity [17].

In this study, a chemical activation method was used to overcome the limitations of thermal regeneration. The spent ACs from WWTP were regenerated by KOH chemical activation, and compared to regenerated ACs using the thermal method. Increased surface area of spent ACs using thermal regeneration was highly dependent on the adsorbed materials on the carbon surface and reaction conditions. However, during chemical activation, the chemical agent reacted with carbons on the surface and pores, and was not significantly affected by the adsorption materials. Similarly, previous research has investigated the chemical regeneration of spent ACs using the reaction between chemical and adsorbed materials [18], but the chemical activation carried out in this study used the reaction between chemical agent and surface carbons at the high temperature. In our knowledge, the regeneration of spent ACs using KOH chemical activation was not published previously. The KOH activation of activated carbon was common and widely investigated, but the regeneration of ACs using KOH activation is a new concept. In addition, the generated ashes on regenerated ACs were removed by the acid treatment, and then the surface area and pore size distributions were compared with the regeneration ACs without the treatment. The final products generated in this study exhibit enough surface area to use the volatile organic compounds (VOC) adsorption facility for purifying the air, which usually requires relatively higher surface area (<1500 m^2/g). Thus, the regenerated ACs were used for adsorption tests of toluene, which is representative chemical of VOCs, and compared with the fresh ACs. The cost of produced ACs usually dependent on the surface area, so the ACs with high surface areas are expensive. The regeneration of ACs with high surface areas is to create high value-added products using the waste.

2. Materials and Methods

2.1. Preparation of Regenerated ACs

PACs are usually used in final stage of WWTP. The spent ACs were collected from a WWTP located in Incheon, Korea. Spent ACs were denoted as S-AC. The S-ACs were dried in an oven at 100 °C overnight prior to use. First, the dried S-AC were thermally regenerated at 850 °C for 3 h [19,20]. Approximately 10 g of S-ACs were placed into the vertical furnace and gradually heated at 5 °C/min until the furnace reached 850 °C. The thermally heated ACs were referred to as H-ACs. The S-ACs also were chemically activated using potassium hydroxide (KOH) pellets (Samchun Chem. Co., 95%). The KOH was kept in a sealed container to prevent air moisture prior to use. A 5 g sample of S-ACs was mixed with 10 g of KOH, and placed into the vertical furnace. The sample was heated from room temperature to 750 °C for 1 h, and then 850 °C for 3 h with a heating rate of 5 °C/min under N_2 flow. The chemically activated S-ACs were then divided into two samples. One sample was washed with 500 mL of tap water, with the process repeated five times. The sample was the chemically activated and then washed by water, so it was denoted as C-AC-W (Chemical activated-AC-Water wash). The second sample was treated with 500 mL of 0.5 M acetic acid (CH_3COOH, Samchun Chem.

Co., 99.5%), and then washed with 500 mL of water three times. It was called by C-AC-A (Chemical activated-AC-Acid wash) in this study.

2.2. Characterization of Prepared ACs

The specific surface areas and pore size distributions of S-AC, H-AC, C-AC-W, and C-AC-A were analyzed using the Brunauer-Emmett-Teller (BET) and NLDFT/GCMC Method based on the N_2 adsorption obtained at 77 K using an BELSORP-max (BEL Japan, Inc.). The content of oxygen functional groups on the surface of each sample was confirmed by X-ray photoelectron spectroscopy (XPS, PHI 5000 VersaProbe, Japan). Elemental analysis (EA) was performed for 12 min at 900 °C using an elemental analyzer (FlashEA 1112 and 2000, Thermo Scientific, Milan, Italy) to determine the elemental contents of carbon (C), hydrogen (H), oxygen (O), nitrogen (N), and sulfur (S). The materials adsorbed on the ACs were analyzed by X-ray fluorescence (XRF-1800, Shimadzu, Japan). For the proximate analysis, dried samples were placed in the furnace (Furnace, Daeheung science, DF-4S) and heated at 950 °C for 7 min, and then lowered to 750 °C for 10 h. The analysis was using the ASTM standard method [21]. The results, including the ash, volatile, and fixed-carbon contents within the ACs, were considered as percentages of the weight [22].

2.3. Test for Adsorption of Toluene on the ACs

The adsorption of toluene on ACs was studied in the tubular quartz reactor with an inner diameter of 3 cm. 200 mg of ACs (W_{ACs}) was put into the reactor and placed between the ceramic fibers (Cerakwool, ©KCC Co., Korea). As shown in Figure 1, the toluene was evaporated through N_2 bubbling and the again diluted by N_2 for controlling its concentration. The concentration of diluent toluene was 400 ppm approximately, and the total flow was 1 L/min. The concentration of toluene was analyzed using THC analyzer with FID detector (Polaris FID, PF-200, Italy). Since the outlet concentration of toluene was the same as the initial concentration, toluene was fully saturated on ACs.

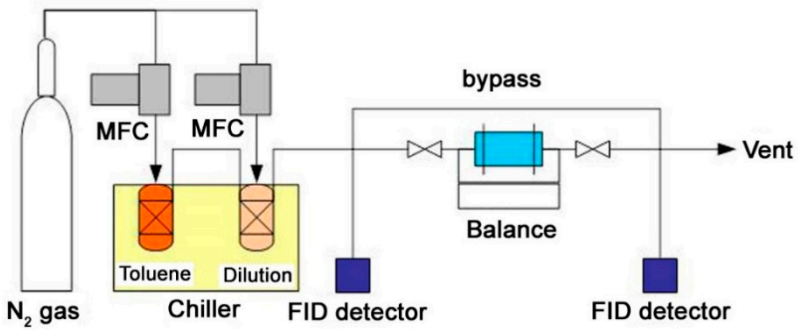

Figure 1. Schematic of experimental setup used for performing adsorption test.

3. Results and Discussion

N_2 adsorption and desorption isotherms of all the curves for S-AC, H-AC, C-AC-W, and C-AC-A at 77 K followed the type IV isotherms (Figure 2a) [23]. In addition, the empty symbols, which depict desorption curves (Figure 2a), had a slightly different pattern with adsorption. As shown in Figure 2b, the pore size distribution of ACs micropore clearly mixed the micropore and mesopores [24].

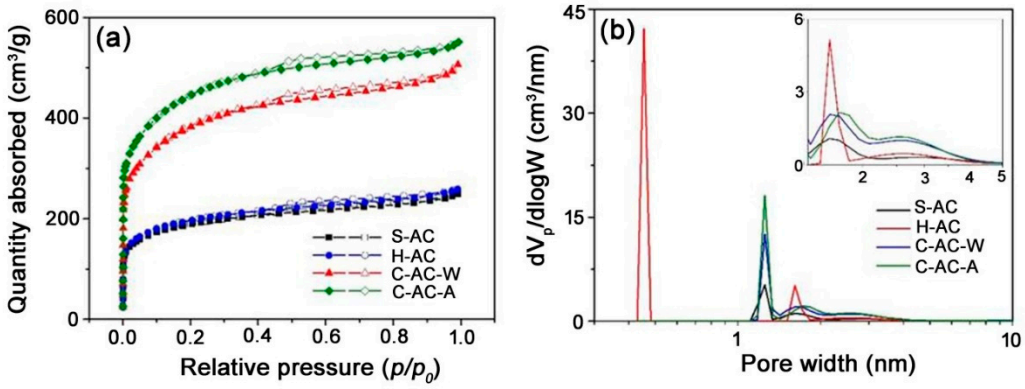

Figure 2. Nitrogen adsorption and desorption isotherms (**a**) and pore size distribution (**b**) of S-AC, H-AC, C-AC-W, and C-AC-A. Solid and empty symbols represent nitrogen adsorption and desorption, respectively.

The quantity absorbed in the y-axis was dependent on the specific surface area. The N_2 adsorption quantity of H-AC was slightly higher than that of S-AC, which means the surface area rarely increased, even when thermally treated. The volatile compounds adsorbed on the carbon surface could be removed by the thermal treatment, but the surface area slightly increased. This is because the volatiles within the pores evaporated, while the pores simultaneously shrunk (Figure 2b). With the exception of H-AC, the pores of the ACs existed between 1–3 nm. The pores of H-ACs were distributed between 0.4–0.5 nm and 1–2 nm. This suggests that the pores of H-ACs shrunk, leading to a lower surface area.

Both chemically activated S-ACs had an absorbed quantity higher than that of S-AC and H-AC, indicating that the both C-ACs have larger surface area compared to others. The surface area could be increased by the broken particles through the chemical activation, leading to the large surface areas. However, the increase of surface area in this study is mainly caused by the increase of total pore volume as shown in Table 1. When the N_2 adsorption of C-AC-W and -A was compared, the C-AC-A adsorption was higher than that of C-AC-W. This indicates that the acid treatment of chemically activated ACs effectively removed the generated ashes and the remained chemical agents used in the chemical activation method. The acid treatment removed the ashes and clear the pores, leading to the increase of surface area and pore volume increase simultaneously (Table 1).

Table 1. Textural properties of the S-AC, H-AC, C-AC-W, and C-AC-A.

	S-AC	H-AC	C-AC-W	C-AC-A
Specific surface area (m^2/g)	681 ± 20	709 ± 18	1383 ± 16	1612 ± 9
Total pore volume (cm^3/g)	0.38 ± 0.06	0.40 ± 0.06	0.78 ± 0.04	0.85 ± 0.03

The C 1 s XPS spectrum, along with the de-convoluted peaks of prepared ACs included C-H, C-C, C-O, C=O, and O-C=O, and π-π bonding at 283.6–284.2, 284.6–284.8, 285.5–285.6, 286.7–286.8, 288.8–289.0, and 290.6–291.1 eV, respectively (Figure 3) [25,26]. When compared with S- and H-AC (Figure 3 a,b), the peaks of H-AC rarely changed, even when they were thermally treated. However, the peaks of chemically activated ACs were significantly different (Figure 3c,d). The concentration of the C-H peak in C-AC-W increased due to the non-graphitic carbonaceous species generated during the chemical activation. Consequently, the carbonaceous species were removed by the acid treatment, resulting in the disappearance of the peaks (Figure 3d) [27]. C-O and COOH peaks in XPS curves were observed to decrease and increase, respectively, after KOH chemical activation of ACs [28]. In this study, the peaks related to the C-O and O-C=O also decreased and increased, respectively, after the chemical activation (Figure 3c,d; Table 2).

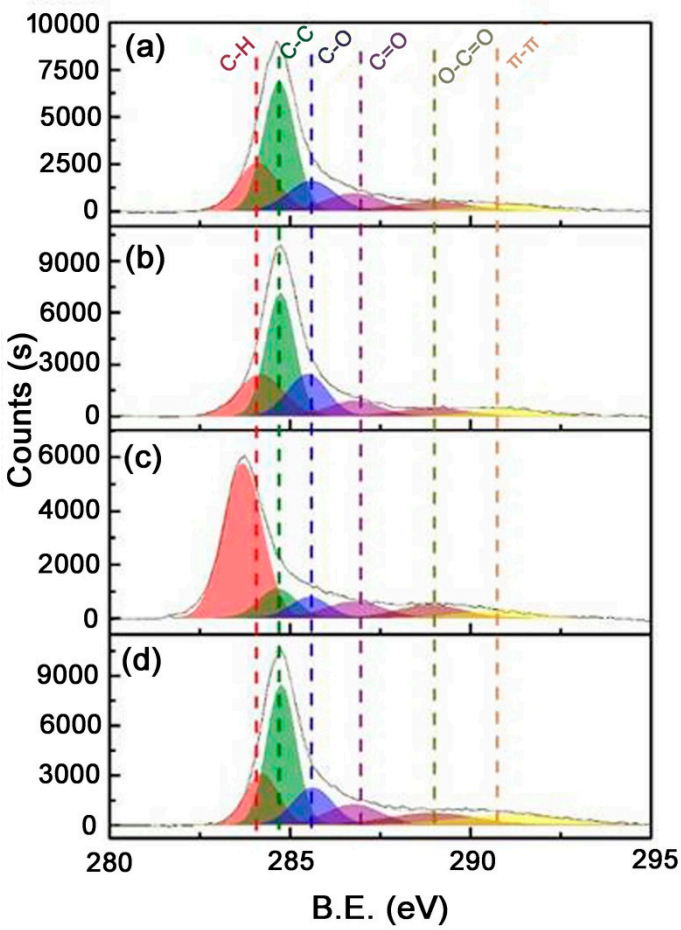

Figure 3. X-ray photoelectron spectroscopy analysis of (**a**) S-AC, (**b**) H-AC, (**c**) C-AC-W, and (**d**) C-AC-A.

Table 2. Relative concentration of different groups in C 1 s peak based on X-ray photoelectron spectroscopy.

B.E. (eV) (Assign)	Surface Concentration (from C 1 s Peak) of (% at.):					
	283.6–284.2	284.6–284.8	285.5–285.6	286.7–286.8	288.8–289.0	290.6–291.1
	(C-H)	(C-C)	(C-O/C-O-C)	(C=O)	(O-C=O)	(π-π)
S-AC	20.14	42.70	14.46	10.39	7.41	4.89
H-AC	21.13	39.57	18.69	8.85	6.55	5.21
C-AC-W	58.51	10.69	7.86	9.32	8.42	5.21
C-AC-A	16.01	39.25	14.20	10.60	9.87	10.08

After thermal treatment, the oxygen content of S-AC sharply decreased. The oxygen containing group was eliminated during the heat treatment. However, the ACs subjected to the chemical activation increased oxygen content due to the carbon oxidization. The total of analysis resulted in the chemically activated ACs were similar with S-AC and H-AC, but the C-AC-A differed (Table 3). The elements without nitrogen, carbon, hydrogen, sulfur, and oxygen could be assumed to be ash. Approximately 14% of total of C-AC-A increased compared to C-AC-W, meaning that ash was reduced by the acid treatment.

Table 3. Elemental analysis (EA) of prepared ACs.

	Elemental Analysis (wt. %)					
	Nitrogen	**Carbon**	**Hydrogen**	**Sulfur**	**Oxygen**	**Total**
S-AC	N.D.	69.98	0.38	N.D.	2.27	72.64
H-AC	N.D.	73.43	0.33	N.D.	0.84	74.60
C-AC-W	N.D.	71.30	0.34	N.D.	3.47	75.12
C-AC-A	N.D.	86.26	0.11	N.D.	2.30	88.68

Analysis condition: dry basis. N.D.: not detected.

The ash removal was also confirmed by the proximate analysis as shown in Figure 4. The ash content of S-ACs was 30%, which was slightly reduced through the thermal treatment and chemical activation. In particular, the ash content of C-AC-A was sharply reduced. The contents of C-AC-A was similar to the commercial ACs (especially coal-based ACs) [29]. Therefore, this suggests that the most physical properties of C-AC-A were recovered as fresh ACs.

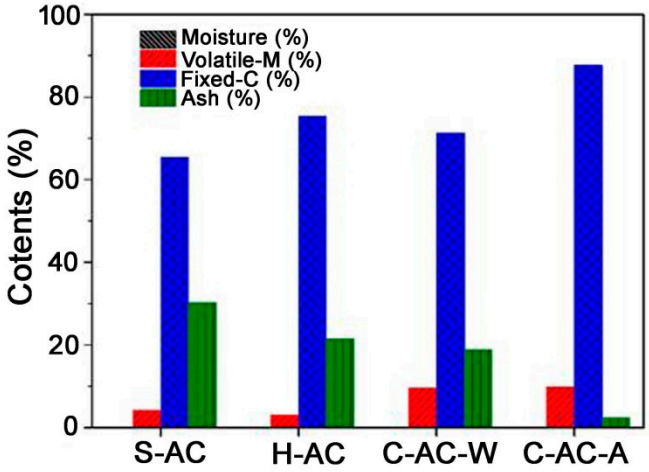

Figure 4. Proximate analysis of the ACs of S-AC, H-AC, C-AC-W, and C-AC-A.

The ashes usually were generated from metal ions in the waste water. The S-ACs were collected in the final process of WWTP. During this process, the various metal ions were adsorbed on the AC surfaces, so the water was purified. The adsorbed metal ions were not evaporated during both thermal treatment and chemical activation, and remained on the carbon surface and pores. The metal ions were converted into the ashes, which blocked the pores and covered the active carbon surface [17]. They reduced the surface area and also prohibited the utilization of ACs. The adsorbed metal ions were analyzed by XRF (Figure 5; Table 4). The Ca, Si, and Fe ions were mainly occupied on the S-ACs. In the H-ACs and C-AC-W, the metal composition was not significantly different. However, the composition and amount of metals changed in C-AC-A. In particular, Ca and Si were reduced compared to the others groups. Acetic acid (CH_3COOH) could dissolve metal ions, including Ca and Si, changing the metal composition and reducing ash content as shown in Figure 5.

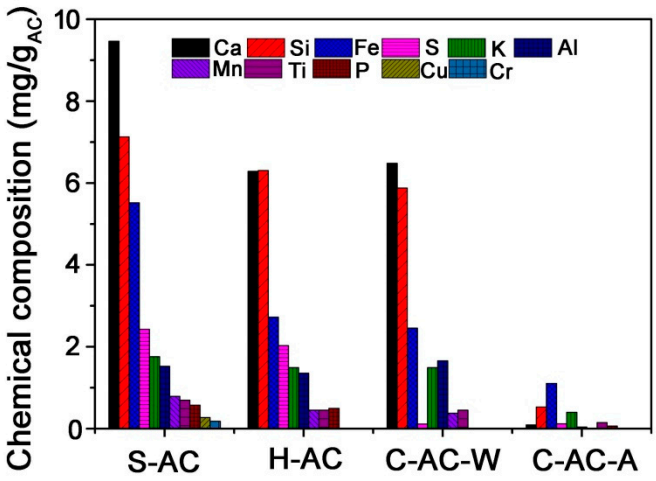

Figure 5. X-ray fluorescence (XRF) analysis of the chemical composition of ACs.

Table 4. Summarized XRF analysis of the ash of ACs.

	XRF Analysis Results (wt. %)										
	Ca	**Si**	**Fe**	**S**	**K**	**Al**	**Mn**	**Ti**	**P**	**Cu**	**Cr**
S-AC	31.2	23.5	18.2	8.0	5.8	5.02	2.6	2.3	1.9	0.9	0.6
H-AC	29.1	29.2	12.6	9.4	6.9	6.27	2.1	2.1	2.3	0	0
C-AC-W	34.3	31.1	13.0	0.6	7.9	8.77	2.0	2.4	0	0	0
C-AC-A	3.7	21.2	44.2	4.8	16.0	1.6	0	6.0	2.6	0	0

The regeneration of S-ACs using the KOH chemical activation increased the specific surface area, which was comparable to the fresh ACs. However, the metal ions present during the water purification process were adsorbed on the ACs and then converted to ashes. The generated ashes were not eliminated through the thermal treatment and chemical activation, leading to the negative effects. The ash removal was essentially required, and the acid washing shown in this study would be suggested.

The toluene adsorption capacities on the ACs were measured using the experimental setup as shown in Figure 1. The surface area, pore size, and functional groups on the surfaces of ACs are considered as key factors to affect adsorption mechanisms, leading to the various toluene adsorption performance [30–33]. First, the toluene adsorption capacities were largest at a higher surface area: C-AC-A > C-AC-W ≈ H-AC > S-AC, and the calculated adsorption capacity was 0.154, 0.091, 0.100, and 0.033 g-$_{toluene}$/g-$_{AC}$, respectively (Table 5). The toluene adsorption capacity calculated the integrated area divided by sample weight. In the previous reports [30,31], pore size distribution is also a key parameter to control the toluene adsorption. The toluene is usually adsorbed on the mesopore of ACs, and then diffused into the micropores. The mixture structure of micro- and meso-pores enhances their toluene adsorption capacity. If the pores are composed of only microstructures or too narrow, the adsorption capacity is decreased. The pores of ACs by chemical activation (C-AC-A) were composed of micropores (pore diameter <2 nm) and meso-pores (2 nm <pore diameter <50 nm) as shown Figure 2b, so it enhanced the toluene adsorption capacity. In addition, the functional group on the ACs can affect the toluene adsorption [33]. The ACs with low content in oxygen surface groups have the best adsorption capacities for VOCs. Based on our EA result in Table 3, the S-AC exhibited high content in oxygen surface groups compared with H-AC. It caused to the significantly low toluene capacity, even comparing with their surface areas. The commercial AC based on coal (889 m^2/g) was prepared, and also applied to the toluene adsorption test. The calculated adsorption capacity was 0.142 g-$_{toluene}$/g-$_{AC}$. The toluene adsorption capacity of C-AC-A is higher than commercial ACs. Therefore, the regenerated ACs from the waste in this study exhibits better physical properties

than commercial ACs, leading to the replacement of fresh ACs. It gives the environmental and economic benefits.

Table 5. Toluene adsorption capacity of prepared ACs.

	S-AC	H-AC	C-AC-W	C-AC-A	Commercial AC
Toluene Capacity ($g\text{-}_{toluene}/g\text{-}_{AC}$)	0.033	0.100	0.091	0.154	0.142

4. Conclusions

The spent activated carbons (S-ACs) from WWTP were regenerated by heat treatment and KOH chemical activation. The specific surface area was increased by thermal regeneration (H-AC), but it was highly increased using the chemical activation (C-AC). The surface area of activated ACs was comparable to the fresh ACs, but ashes generated during this process caused issued for regenerated ACs. The ashes initially accumulated during the water purification process. The metal ions were adsorbed on the ACs, and then converted into ashes. The accumulated ashes blocked the pores and covered the surface, leading to the negative effects. The chemically activated ACs were washed by acetic acid (C-AC-A) and compared to the ACs without acid washing (C-AC-W). The ACs with acid washing increases 17% in available surface area, and the pore volume also increased. The C-AC-A was applied for toluene adsorption. The toluene adsorption capacity of C-AC-A was even higher than the commercial ACs. The quality of regenerated ACs was improved comparing with the commercial ACs, so it could replace the fresh ACs. Hence, the regenerated ACs preserve the environment and provide benefits to the industries.

Author Contributions: Conceptualization, validation, investigation, writing—original draft preparation, review and editing, J.E.P. and S.Y.H.; methodology, and software, and data curation, G.B.L.; formal analysis, S.Y.H.; resources, supervision, project administration, and funding acquisition, B.U.H.

Funding: This subject is supported by Korean Ministry of Environment (Project No. 201902014) and the Korea Agency for Infrastructure Technology Advancement (KAIA) grant funded by the Ministry of Land, Infrastructure and Transport (Grant 19IFIP-B113506-04).

Conflicts of Interest: The authors declare no conflict of interest.

References

1. Luo, Y.; Guo, W.; Ngo, H.H.; Nghiem, L.D.; Hai, F.I.; Zhang, J.; Liang, S.; Wang, X.C. A review on the occurrence of micropollutants in the aquatic environment and their fate and removal during wastewater treatment. *Sci. Total Environ.* **2014**, *473*, 619–641. [CrossRef]
2. Thellmann, P.; Greiner-perth, K.; Jacob, S.; Knoll, M.; Schäfer, M.; Stängle, M.; Ziegler, M.; Scheurer, M.; Köhler, H.R.; Triebskorn, R. Does Waste Water Treatment Plant Upgrading with Powdered Activated Carbon Result in Reduced Water and Sediment Toxicity of the Receiving Stream? *Int. Water Wastewater Treat.* **2017**, *3*, 2.
3. San Miguel, G.; Lambert, S.D.; Graham, N.J.D. The regeneration of field-spent granular-activated carbons. *Water Res.* **2001**, *35*, 2740–2748. [CrossRef]
4. Moona, N.; Murphy, K.R.; Bondelind, M.; Bergstedt, O.; Pettersson, T.J.R. Partial renewal of granular activated carbon biofilters for improved drinking water treatment. *Environ. Sci. Water Res. Technol.* **2018**, *4*, 529–538. [CrossRef]
5. Sabio, E.; González, E.; González, J.F.; González-García, C.M.; Ramiro, A.; Gañan, J. Thermal regeneration of activated carbon saturated with p-nitrophenol. *Carbon N. Y.* **2004**, *42*, 2285–2293. [CrossRef]
6. Bhagawan, D.; Poodari, S.; Ravi kumar, G.; Golla, S.; Anand, C.; Banda, K.S.; Himabindu, V.; Vidyavathi, S. Reactivation and recycling of spent carbon using solvent desorption followed by thermal treatment (TR). *J. Mater. Cycles Waste Manag.* **2014**, *17*, 185–193. [CrossRef]
7. Ledesma, B.; Román, S.; Álvarez-Murillo, A.; Sabio, E.; González-García, C.M. Fundamental study on the thermal regeneration stages of exhausted activated carbons: Kinetics. *J. Therm. Anal. Calorim.* **2014**, *115*, 537–543. [CrossRef]

8. Cazetta, A.L.; Junior, O.P.; Vargas, A.M.M.; Da Silva, A.P.; Zou, X.; Asefa, T.; Almeida, V.C. Thermal regeneration study of high surface area activated carbon obtained from coconut shell: Characterization and application of response surface methodology. *J. Anal. Appl. Pyrolysis* **2013**, *101*, 53–60. [CrossRef]
9. Guo, Y.; Du, E. The Effects of Thermal Regeneration Conditions and Inorganic Compounds on the Characteristics of Activated Carbon Used in Power Plant. *Energy Procedia* **2012**, *17*, 444–449. [CrossRef]
10. Çalişkan, E.; Bermúdez, J.M.; Parra, J.B.; Menéndez, J.A.; Mahramanlioğlu, M.; Ania, C.O. Low temperature regeneration of activated carbons using microwaves: Revising conventional wisdom. *J. Environ. Manag.* **2012**, *102*, 134–140. [CrossRef]
11. Berenguer, R.; Marco-Lozar, J.P.; Quijada, C.; Cazorla-Amorós, D.; Morallón, E. Comparison among chemical, thermal, and electrochemical regeneration of phenol-saturated activated carbon. *Energy Fuels* **2010**, *24*, 3366–3372. [CrossRef]
12. Álvarez, P.M.; Beltrán, F.J.; Gómez-Serrano, V.; Jaramillo, J.; Rodríguez, E.M. Comparison between thermal and ozone regenerations of spent activated carbon exhausted with phenol. *Water Res.* **2004**, *38*, 2155–2165. [CrossRef] [PubMed]
13. Bagreev, A.; Rahman, H.; Bandosz, T.J. Thermal regeneration of a spent activated carbon previously used as hydrogen sulfide adsorbent. *Carbon N. Y.* **2001**, *39*, 1319–1326. [CrossRef]
14. Kapteijn, F.; Porre, H.; Moulijn, J.A. CO_2 gasification of activated carbon catalyzed by earth alkaline elements. *AIChE J.* **1986**, *32*, 691–695. [CrossRef]
15. Salvador, F.; Sánchez Jiménez, C. Effect of regeneration treatment with liquid water at high pressure and temperature on the characteristics of three commercial activated carbons. *Carbon N. Y.* **1999**, *37*, 577–583. [CrossRef]
16. Perry, L.; Essex, D.; Giess, P.; Graham, N.; Kaur, K.; Lambert, S.; Spencer, C. Improving the performance of granular activated carbon (GAC) via pre-regeneration acid treatment. *Water Environ. J.* **2005**, *19*, 159–166. [CrossRef]
17. Kim, S.-G.; Son, H.-J.; Jung, J.-M.; Ryu, D.-C.; Yoo, P.-J. Evaluation of Drinking Water Treatment Efficiency according to Regeneration Temperatures of Granular Activated Carbon (GAC). *J. Environ. Sci. Int.* **2015**, *24*, 1163–1170. [CrossRef]
18. Newcombe, G.; Drikas, M. Chemical regeneration of granular activated carbon from an operating water treatment plant. *Water Res.* **1993**, *27*, 161–165. [CrossRef]
19. Park, J.E.; Lee, G.B.; Hwang, S.Y.; Kim, J.H.; Hong, B.U.; Kim, H.; Kim, S. The effects of methane storage capacity using upgraded activated carbon by KOH. *Appl. Sci.* **2018**, *8*, 1596. [CrossRef]
20. Lee, G.B.; Park, J.E.; Hwang, S.Y.; Kim, J.H.; Kim, S.; Kim, H.; Hong, B.U. Comparison of by-product gas composition by activations of activated carbon. *Carbon Lett.* **2019**, *29*, 263–272.
21. Basu, P. *Biomass Gasification, Pyrolysis and Torrefaction*; Elsevier: Amsterdam, The Netherlands, 2018; pp. 479–495.
22. Nunes, L.J.R.; De Oliveira Matias, J.C.; Da Silva Catalão, J.P. *Torrefaction of Biomass for Energy Applications*; Elsevier: Amsterdam, The Netherlands, 2018; pp. 1–43.
23. Manocha, S.M. Porous carbons. *Sadhana* **2003**, *28*, 335–348. [CrossRef]
24. Zhang, Y.; Shao, D.; Yan, J.; Jia, X.; Li, Y.; Yu, P.; Zhang, T. The pore size distribution and its relationship with shale gas capacity in organic-rich mudstone of Wufeng-Longmaxi Formations, Sichuan Basin, China. *J. Nat. Gas Geosci.* **2016**, *1*, 213–220. [CrossRef]
25. Barroso-Bogeat, A.; Alexandre-Franco, M.; Fernández-González, C.; Gómez-Serrano, V. Activated carbon surface chemistry: Changes upon impregnation with Al(III), Fe(III) and Zn(II)-metal oxide catalyst precursors from NO3− aqueous solutions. *Arab. J. Chem.* **2016**. [CrossRef]
26. Zhang, L.; Tu, L.; Liang, Y.; Chen, Q.; Li, Z.; Li, C.; Wang, Z.; Li, W. Coconut-based activated carbon fibers for efficient adsorption of various organic dyes. *Rsc. Adv.* **2018**, *8*, 42280–42291. [CrossRef]
27. Datsyuk, V.; Kalyva, M.; Papagelis, K.; Parthenios, J.; Tasis, D.; Siokou, A.; Kallitsis, I.; Galiotis, C. Chemical oxidation of multiwalled carbon nanotubes. *Carbon N. Y.* **2008**, *46*, 833–840. [CrossRef]
28. Ibrahim Abouelamaiem, D.; Mostazo-López, M.J.; He, G.; Patel, D.; Neville, T.P.; Parkin, I.P.; Lozano-Castelló, D.; Morallón, E.; Cazorla-Amorós, D.; Jorge, A.B.; et al. New insights into the electrochemical behaviour of porous carbon electrodes for supercapacitors. *J. Energy Storage* **2018**, *19*, 337–347. [CrossRef]
29. Dabrowski, A.; Podkościelny, P.; Hubicki, Z.; Barczak, M. Adsorption of phenolic compounds by activated carbon—A critical review. *Chemosphere* **2005**, *58*, 1049–1070. [CrossRef]

30. Lim, S.T.; Kim, J.H.; Lee, C.Y.; Koo, S.; Jerng, D.-W.; Wongwises, S.; Ahn, H.S. Mesoporous graphene adsorbents for the removal of toluene and xylene at various concentrations and its reusability. *Sci. Rep.* **2019**, *9*, 10922. [CrossRef]
31. Hwang, S.Y.; Lee, G.B.; Park, J.E.; Kim, J.H.; Kim, S.; Hong, B. Removal and recycling of volatile organic compounds (VOCs) adsorbed on activated carbons using in situ vacuum systems. *Int. J. Environ. Sci. Technol.* **2019**, *16*, 7827–7836. [CrossRef]
32. Lillo-Ródenas, M.A.; Cazorla-Amoró, D.; Linares-Solano, A. Behaviour of activated carbons with different pore size distributions and surface oxygen groups for benzene and toluene adsorption at low concentrations. *Carbon N. Y.* **2005**, *43*, 1758–1767.
33. Chiang, Y.C.; Chiang, P.C.; Huang, C.P. Effects of pore structure and temperature on VOC adsorption on activated carbon. *Carbon N. Y.* **2001**, *39*, 523–534. [CrossRef]